Eastern Europe Conference on Timber Constructions

Optimisation of connections by increasing friction in the shear plane

Simon Aurand[1]

ABSTRACT: As part of a research project, connections were optimised by increasing the friction in the shear plane through surface modification. Therefore, many different surface modification processes were initially analysed and tested for their applicability, especially on an industrial scale. The various surfaces were quantified by friction tests and both static and kinetic coefficients of friction were determined. It was found that surfaces with uniform, even structuring are preferable to surfaces with strong, punctual structuring. The first step was to identify suitable surface finishes by means of push-out tests. Further connection tests were then carried out with these surfaces to investigate the behaviour of inclined screws and increased friction in the shear plane. This enabled group effects such as block shear failure to be investigated and ruled out and new types of failure, such as transverse compression failure under the connector plates, to be identified. Increases in load-carrying capacity of up to 43 % and increases in stiffness of up to 29 % were determined due to increased friction in the shear plane. Using an analytical calculation model, the load-carrying capacity of the connection could be determined well and the evaluation of the results showed that the static coefficient of friction determines both the average load-carrying capacity and the characteristic load-carrying capacity well. Fatigue tests to determine the long-term behaviour of connections with inclined screws and increased friction in the shear plane showed that the friction is still activated even after a longer period of time and participates in the load transfer.

KEYWORDS: surface modification, friction, shear plane, inclined screws, connections

1 INTRODUCTION

1.1 Connections with inclined screws and system connectors

Timber structures are becoming increasingly larger and more complex. This means that existing connections need to be optimised for higher load-carrying capacities to withstand the increasing forces. At the same time, construction is becoming more expensive. This is reflected in rising personnel and labour costs [1] and rising material costs [2]. The construction industry must therefore manage to build more resource-efficiently. This in turn requires the optimisation of existing connections to reduce material requirements. This paper has already been presented at the *Karlsruher Tage Holzbau 2024* in slightly modified form.

The connections described here are so-called system connectors. System connectors are an economical connection due to their high degree of prefabrication. The connector plates (usually milled from aluminium or steel) are attached to the timber components in the factory and then only need to be inserted into each other on site. When fastening the connector plates to the timber, a distinction is made between two screw arrangements: firstly, fully threaded screws inserted perpendicular to the shear plane, and secondly, screws that are inserted into the timber at an angle to the grain (see Figure 1).

This second case, with the screws inclined at an angle, is considered in more detail: Under load parallel to the shear plane, the screws are almost exclusively subjected to tensile load [3]. The force diagram can be seen in Figure 2.

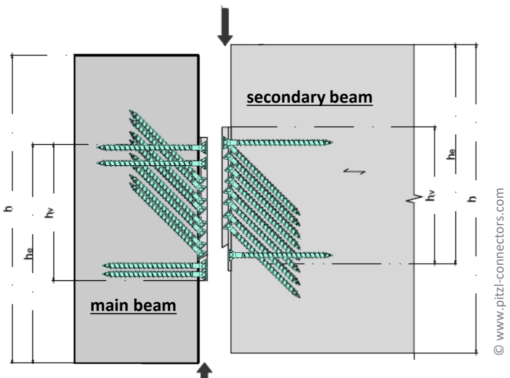

Figure 1: *Fastening of system connectors.*

For equilibrium reasons, there is a force component perpendicular to the shear plane. This force perpendicular to the shear plane in turn generates a contact pressure in the shear plane and thus activates friction. The friction in turn generates an additional force component parallel to the shear plane, which adds to the load transfer. This is known as the rope effect and is taken into account in Eurocode 5 [4] with a standardised friction coefficient of $\mu = 0.25$.

[1] KIT Timber Structures and Building Construction,
Karlsruhe Institute of Technology (KIT), Karlsruhe, Germany
simon.aurand@kit.edu

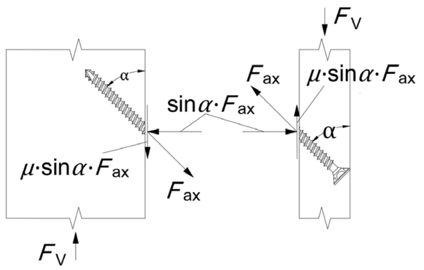

Figure 2: *Force diagram of acting forces in a connection with inclined screws.*

1.2 Friction in the shear plane

As Figure 2 shows, friction occurs in the shear plane and this is involved in the load transfer. This results in the potential to increase the friction in the shear plane by means of an appropriate surface modification and thus to increase the overall load-carrying capacity of the connection. Building on this, the increased friction coefficients should also be able to be used later in the design of such connections. This challenge was to be overcome in two steps. Firstly, the quantification of surface modifications based on the determination of friction coefficients. Based on this, the load-carrying capacities of connections with increased friction in the shear plane were then determined. Secondly, an analytical model should be derived, build on the analytical principles and considering actual failure mechanisms from experimental tests.

2 MATERIAL AND METHODS

2.1 Surface modifications

To increase the friction in the shear plane between the connector and the softwood and thus to increase the load-carrying capacity of a subsequent connection through an increased rope effect, various types of surface modification were investigated on different materials. The materials used were, on the one hand, normal steel sheets in various thicknesses and, on the other hand, most of the surface modifications were carried out with densified veneer wood (DVW). A detailed description of the used DVW can be found in [5]. In [5], all surface modifications with DVW are also presented in detail. Therefore, in this article the surface modifications in steel are presented. All surface modifications have been systematically named according to German standard DIN 8580 *Manufacturing processes* [6] and categorised into three main groups (see Figure 3). The manufacturing processes in the three main groups carried out on steel specimens are presented below.

2.1.1 Forming

Notching

During notching, the material is cold formed using a punching tool. During the tests, workpieces with a file cut (Figure 4a) and rasp cut (Figure 4b) were analysed. These surface modifications are only possible with cold formable materials such as steel or aluminium. The process is currently limited to narrow workpieces. The complexity of the manufacturing process and the fact that it can currently only be used for certain materials and narrow workpieces make it clear that this surface modification is a very complex process.

Embossing

During embossing, a defined pattern is stamped into the surface of the workpiece using an embossing die. In the tests, a conventional chequered plate was examined (Figure 4c), as used for non-slip floor coverings. Once the embossing die has been produced (e.g. by milling), the embossing process is simple, making it a relatively easy way of surface modification of various materials.

Punching

Punching combines the two manufacturing processes of forming and cutting. When punching, the workpiece is simultaneously formed, and material is removed using a punching tool. The punching process is therefore only applicable to (thin) sheet metal. Punched sheets can be produced in large quantities as soon as the punching tool is manufactured with the required properties. A total of three different geometries were investigated. Geometry 1, punched on one side, with a very sharp-edged collar (Figure 4d). Geometry 2, also punched on one side, with a rather flat, round collar (Figure 4e) and geometry 3, punched on both sides with a collar that is also round but has a much sharper edge (Figure 4f).

2.1.2 Parting

Profile milling – circular pattern

Very smooth surfaces can be produced by face milling. However, the result always shows visible trochoidal marks that follow the movement of the milling cutter's cutting edge. If the indexable inserts are removed from the milling tool and the speed is increased, visible and noticeable trochoidal marks remain. This concept was used for the circular pattern, where only two opposing inserts were used on the milling tool. The remaining inserts were removed before milling. The milling tool rotated at a constant high speed and was guided over the surface of the test specimens at a high feed rate.

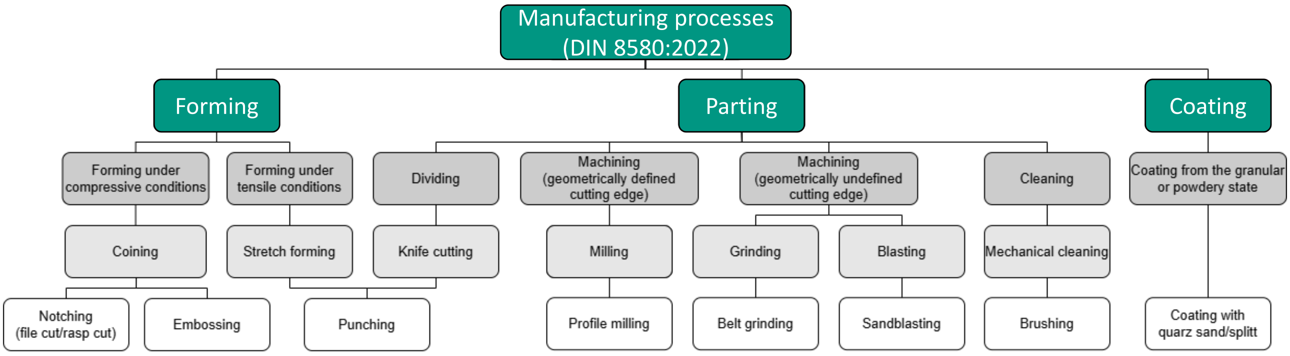

Figure 3: *Classification and naming of the analysed surface finishes.*

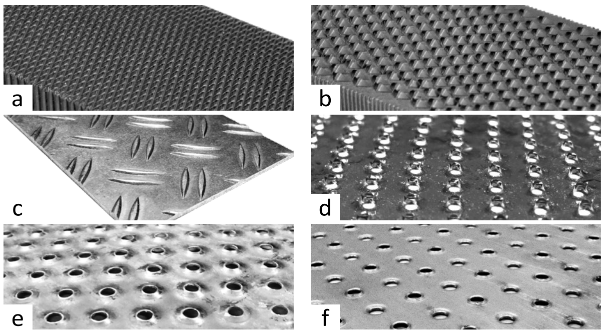

Figure 4: *Surfaces in main group "Forming": (a) file cut, (b) rasp cut, (c) chequered plate, (d) geometry 1 punched on one side, (e) geometry 2 punched on one side, (f) geometry 3 punched on both sides.*

In this way, circular grooves were milled into the top layer of the test specimens, which repeatedly overlapped. The result was pyramid-like shapes at the edge of the test specimens, while elongated grooves were in the centre of the specimens (see Figure 5a). The turning speed and feed rate had a significant influence on the surface quality. The manufacturing process was simple and the manufacturing time short.

Profile milling – micro notches
Parallel grooves were milled into the surface using a finger cutter. The milling cutter was inclined by 5° so that a sharp edge was created. The distance between the grooves was 10 mm, which was significantly larger than the pyramid pattern presented in [5]. Due to the large distance between the grooves, the manufacturing process was fast. Figure 5b shows the surface of a machined steel plate.

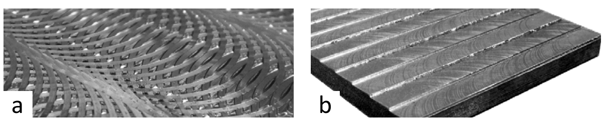

Figure 5: *Surfaces in main group "Parting": (a) circular pattern, (b) micro notches.*

2.1.3 Coating

A flowable two-component epoxy resin was used for the coating, which cured at room temperature. The test specimens were coated with quartz sand with a grain size of 0.5–1.0 mm. The surfaces of the steel test specimens were sandblasted and degreased before the adhesive was applied. A 0.5 mm thick layer of adhesive was selected for the coating (Figure 6) The test specimens were pressed into the respective granulate by hand. The test specimens cured for one week at room temperature in accordance with the manufacturer's instructions.

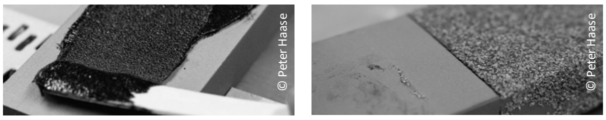

Figure 6: *Surfaces in main group "Coating": (a) viscous 2-component epoxy resin adhesive, (b) coating with quartz sand 0.5–1.0 mm.*

2.2 Friction tests

2.2.1 Test setup and execution

The test setup shown in Figure 7 was used to determine the coefficient of friction (based on [7]). The force F_N perpendicular to the friction surface was applied force-controlled with a hydraulic cylinder. A compressive stress of 2.5 N/mm² was selected for the contact pressure, which corresponds to the characteristic compressive strength perpendicular to the grain of softwood. The softwood used was spruce/fir, which was stored in a standardised climate at 20°C and 65 % RH and had an average wood moisture content of $u = 12$ %. The surfaces were free of knots >5 mm and without glue lines. The force F_R parallel to the friction surface was applied using a universal testing machine. The entire test sequence was carried out at a test speed of 5 mm/min and up to a displacement of 15 mm (displacement of machine head).

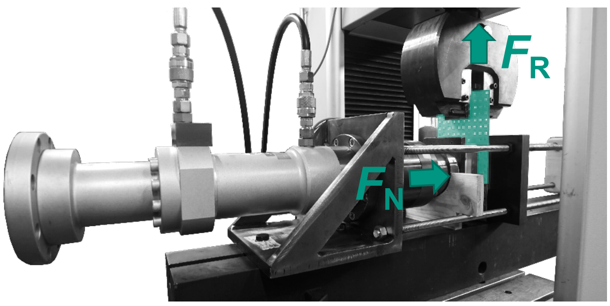

Figure 7: *Test setup for friction tests.*

For this article, tests were carried out to determine the coefficient of friction between softwood and steel/aluminium. In the tests, a distinction was made between the side and end grain of the softwood to cover the different installation situations of the connectors. A distinction was also made as to whether the grain direction of the face grain was parallel or perpendicular to the load direction F_R. The different test configurations can be seen in Figure 8. Side members with a similar density were selected for the tests.

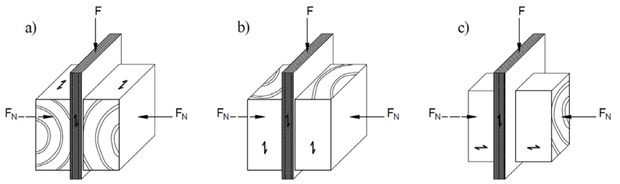

Figure 8: *Friction tests with a) side member perpendicular and b) parallel to the load direction and with c) end grain.*

The coefficient of friction was calculated with Equation (1). The force F_R was divided equally between the two friction surfaces parallel to the contact surface. The static coefficient of friction μ_s and the kinetic coefficient of friction μ_k were analysed.

$$\mu = \frac{F_R}{2 \cdot F_N} \quad (1)$$

2.3 Connection tests

Based on the friction tests, experiments were carried out with connectors made of densified veneer wood (DVW). Initially, many different surface modifications were investigated in connections with inclined screws. The aim was to investigate whether a sufficiently high contact pressure can be generated in the shear plane by inclined screws so that the previously determined static friction coefficients occur. Based on the results, specific surface finishes were identified with which further connection tests were carried out. Initially, connections were made with longer screws to fully utilise the connection by fully utilising the screws (i.e. reaching the tensile strength). Then, by significantly increasing the number of screws, group effects such as block shear failure were investigated. In all tests, the force between the two connector parts was transmitted exclusively via contact pressure.

In series 6a, a first prototype v1 for a connector made of 25 mm thick DVW was developed in collaboration with Pitzl Metallbau GmbH in Altheim. Among other things, the focus was on a milled surface for higher friction in the shear plane. The pyramid pattern with 0.5 mm deep pyramids was selected for the surface modification. Based on the results, a second prototype v2 was produced and tested in series 6b. This time, the pyramid pattern with 1.0 mm deep pyramids was selected for the surface. For both prototypes and all tests, Würth ASSY 4 plus 6x200 mm fully threaded screws were used, which were inclined at 45° to the shear plane.

In series 7, a prototype for a heavy-duty connector for loads of up to 500 kN was manufactured and tested. The connector parts were milled from 50 mm thick, cross-laminated DVW. The pyramid pattern with 1.0 mm deep pyramids was milled into the surface. The fully threaded screws were Würth ASSY 4 plus 8x300 mm, also inclined at 45° to the shear plane. A total of 20 screws per connector plate were arranged in five rows. An overview of the tests carried out is given in Table 1.

Table 1: *Overview of push-out tests carried out.*

series	no. of tests	no. of screws*	screws *d* x *L*	connector** *W* x *H* x *D*
	-	-	mm	mm
1	3	5	5x100	110x58x15
2	5	5	5x100	110x58x25
3	5	5	6x180	110x58x25
4	5	15	6x100	110x150x25
5	3	15	6x200	110x150x25
6a	8	10	6x200	110x100x25
6b	7	12	6x200	110x100x25
7	5	20	8x300	140x254x50

* per shear plane
** size of one connector plate

2.3.1 Test setup and execution

The test setup is shown in Figure 9 The surfaces of the DVW connectors were only modified on one side and fastened to the side and middle members with inclined screws. Fully threaded screws were chosen for all rows.

The test specimens were loaded with a universal testing machine. During the tests, both the machine load and the relative displacement between the middle and side members were measured. The relative displacement of the individual connections was measured at the front and rear of the test specimens. The tests were carried out and analysed in accordance with EN 26891 [10]. Both the maximum load $F_{V,test}$ and the stiffness k_s per connector and shear plane were determined. The stiffness was determined in the linear-elastic range between 10 % and 40 % of the maximum load.

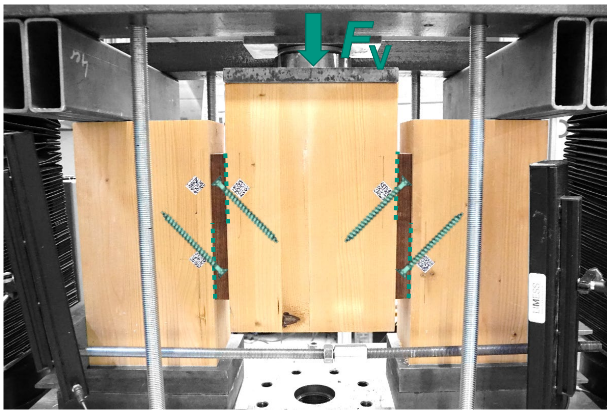

Figure 9: *Test setup for the push-out tests with inclined screws.*

2.4 Analytical model

In [5], a model was presented to calculate the load-carrying capacity in the insertion direction $F_{V,exp}$ of a connection with inclined screws, see equation (2). Input values for the model include the minimum of the withdrawal capacity and the tensile load capacity of the screws as well as the maximum coefficient of friction in the shear plane. Based on the results of the connection tests, the compressive load-carrying capacity perp. to the grain of the softwood below the connector plates must be checked when designing connections with inclined screws and increased friction in the shear plane. Due to the large number of screws in a small area, very high stresses arise locally under the connector plates perpendicular to the grain. The load-carrying capacity of the connector plates themselves must also be taken into account in order to avoid failure in the net cross-section.

The total load-carrying capacity of the connection with inclined screws is, therefore, the minimum from equation (2). The first two lines take into account the withdrawal capacity on the one hand and the tensile load-carrying capacity of the screws on the other. Line three takes into account the failure of the main beam under compression perpendicular to the grain and line four takes into account the failure of the connector itself (here compression in grain direction).

$$F_V = \min \begin{cases} n_{ef} \cdot F_{ax} \cdot (\mu \cdot \sin\varepsilon + \cos\varepsilon) \\ n_{ef} \cdot F_{tens} \cdot (\mu \cdot \sin\varepsilon + \cos\varepsilon) \\ A_{c,90,header} \cdot f_{c,90,header} \cdot k_{c,90,header} \cdot \left(\mu + \dfrac{1}{\tan\varepsilon} \right) \\ A_{nett,connector} \cdot f_{c,0,connector} \end{cases} \quad (2)$$

with

n_{ef}	effective number of fasteners
F_{ax}	withdrawal capacity of the screw
F_{tens}	tensile capacity of the screw
μ	coefficient of friction
ε	angle of inclination of the screws
$A_{c,90,header}$	area on main beam subjected to compression perpendicular to the grain
$f_{c,90,header}$	compression strength perp to grain
$k_{c,90,header}$	stress spreading factor
$A_{nett,connector}$	nett cross-sectional area of connector
$f_{c,0,connector}$	strength of connector (here compressive strength in grain direction of DVW)

2.5 Long-term behaviour

The increase in the load-carrying capacity of connections with inclined screws is based on increased friction in the shear plane due to the surface modification. It is therefore important that there is sufficient contact pressure in the shear plane for the entire service life of the connection. This raises the question of whether the contact pressure is still present after a longer period and thus whether friction can still be activated. This should be the case, as the screws inclined at an angle to the fibre. This inclination ensures that the screws are always subjected to tensile load, thus creating a compressive force perpendicular to the shear plane (see force diagram in Figure 2). But what happens if the wood shrinks and swells under climatic conditions? This question was investigated in long-term tests. The connections were exposed to different climatic conditions (i.e. service class 1 and 2) under constant load. After a period of more than one year, the test specimens were unloaded, and the residual load-carrying capacity and stiffness were determined.

SC 1 refers to heated interior spaces with an average temperature of 20°C and a relative humidity that only exceeds 65 % for a few weeks of the year. This condition leads to an average wood moisture content of <12 %. SC 2 refers to roofed but open constructions with a relative humidity that only exceeds 85 % for a few weeks of the year. This condition leads to an average wood moisture content of <20 %.

2.5.1 Test setup and execution

The test specimens were produced in a similar way to the short-term tests and can be seen in Figure 10. For the connectors the previously presented prototypes v1 and v2 were used. The connector plates were fastened to the side and middle member made of GL 24h using screws (Würth ASSY 4 plus 6x200 mm) inclined at 45°. The glulam was stored at a normal climate of 20°C and 65 % RH before the tests. The side members were significantly longer than in the short-term tests, so that there were two connector plates on each side timber, one at the top and one at the bottom. A total of four connections were tested with each test specimen. Two test specimens in SC 1 and two in SC 2 were tested. One specimen in each service class contained four connectors v2, and the other specimen in each service class contained two connectors v2 at the top and two connectors v1 at the bottom.

The load was applied via large compression springs and threaded rods. The two middle members were loaded simultaneously and as evenly as possible with springs via steel profiles and large washers. In this way, two push-out tests with four connectors could be tested in each test setup. The compression springs each had a spring force of 50 kN. The constant permanent load was selected at approx. 30 % of the maximum loads determined in the short-time tests (50 kN corresponds to 33 % for connector v2 and 28 % for connector v1). The load of 50 kN per connector corresponds to a characteristic load level of the connectors of 37 % for connector v2 and 33 0% for connector v1. The load level was limited to around 30%, as compression springs were only available with a maximum spring force of 50 kN.

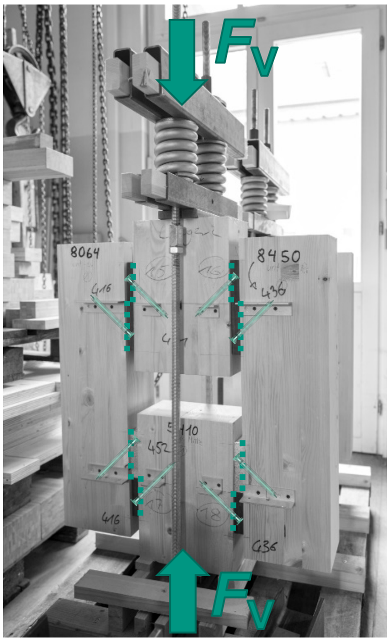

Figure 10: Long-term test setup.

The test specimens were loaded with a universal testing machine up to 100 kN (i.e. 50 kN in each spring), after which the nuts of the threaded rods were tightened to compress the springs at 50 kN. The test specimens were returned to the laboratory after approximately 330 days to check the load on the springs and reload them if necessary. The recorded loads were between 90 and 95 % of the target load. Using a universal testing machine, each test specimen was reloaded to 100 kN. After approx. 570 days, the specimens were unloaded, again using a universal testing machine. The spring forces were no less than 93% of the target load. After unloading and removal of the springs, the specimens were returned to their storage location to recover in their respective climatic environment.

The tests to determine the residual load-carrying capacity and stiffness values were analogous to the short-term tests.

3 RESULTS AND DISCUSSION

3.1 Friction tests

The results of the friction coefficients of all the surface modifications presented here are shown in Figure 11 and listed in Table 2. The results of the tests from [5] are also listed for comparison purposes.

3.1.1 Anodised aluminium

Initially, tests were carried out with anodised aluminium to quantify the results of further surface modifications. The tests were carried out with actual connector plates. The results averaged $\mu_s = 0.30$ for the tests with face grain and $\mu_s = 0.39$ for the tests with end grain. Coefficients of variation (COV) of 13–20% show a high scatter of friction coefficients.

3.1.2 Notched surfaces

The highest coefficients of friction in the main group *Forming* were achieved with the steel plates with file cut and rasp cut. The tests with face grain perpendicular achieved an average of $\mu_s = 1.06$ and $\mu_s = 1.33$ for file and rasp cuts respectively. However, the scatter of the test results was very high with COV of 11–30%. Very good interlocking with the softwood was observed with both surfaces during the tests. No damage was observed on the steel surface with either the file or rasp cut and the great potential of notched surfaces was demonstrated.

3.1.3 Embossed surfaces

The embossed surface of the chequered plate also shows a significant increase in the coefficient of friction for tests with face grain perpendicular with an average value of $\mu_s = 0.59$. Despite a strong indentation of the surface into the softwood, it is evident that protruding surface features must be limited in size to cause an increase in the coefficient of friction, as there is a tendency for the softwood to "roll" over the protruding structure.

3.1.4 Punched surfaces

The three tested punched geometries showed very different values for tests with face grain perpendicular with mean values of $\mu_s = 0.82$, $\mu_s = 0.48$ and $\mu_s = 0.67$ for geometry 1, 2, and 3 respectively. The sheets with geometry 1 (thickness = 0.25 mm) experienced tensile failure of the sheet, therefore the results only represent lower limit values. In the tests with geometry 2, the surface slid along the softwood, which explains the low values. With the sheets of geometry 3, there was strong interlocking with the softwood and damage to it. The sheets themselves, however, showed no damage after the tests.

3.1.5 Milled surfaces

The circular milled pattern showed a significant increase in the coefficient of friction with $\mu_s = 0.64$ for face grain perpendicular compared to aluminium. The micro notches showed a strong increase in the coefficient of friction with $\mu_s = 1.29$, especially in the tests with end grain. In direct comparison with the milled pyramid patterns in the DVW, it could be shown that the larger the structure (increasing milling depth of the pyramids), the greater the coefficient of friction could be determined. On average, values of $\mu_s = 0.84$ (0.5 mm), $\mu_s = 0.94$ (1.0 mm), $\mu_s = 1.06$ (1.5 mm) and $\mu_s = 1.15$ (2.0 mm) were determined in these tests with right-angled face grain.

3.1.6 Coated surfaces

In the tests with the coated test specimens, higher coefficients of friction were also determined, with $\mu_s = 0.68$ for face grain perpendicular, compared to aluminium. Interestingly, the results with the quartz sand were higher than with the split. This confirms the finding of the tests with the chequered plates that the size of the surface features must be limited, otherwise the softwood will "roll" over the surface. The tests also showed that a great deal of effort is required to produce the test specimens and that the surface quality is associated with a high degree of uncertainty.

3.1.7 Mean values and characteristic values

The characteristic values were calculated in accordance with EN 14358 [8] and EN 14545 [9]. A global coefficient of variation COV_g was calculated for the 5%-quantile based on all friction tests. A total of $n = 844$ friction tests were carried out and the global coefficient of variation COV_g was calculated as 0.16. The coefficient $k_s(n)$ was calculated to be 1.76. The results (static coefficient of friction μ_s and kinetic coefficient of friction μ_k) of all surfaces presented and the corresponding characteristic values are given in Table 2.

Table 2: *Overview of friction coefficients: Mean values and characteristic values.*

surface	static coefficient of friction μ_s mean value / characteristic value			kinetic coefficient of friction μ_k mean value / characteristic value		
	FG ∥	FG ⊥	EG	FG ∥	FG ⊥	EG
anodised aluminium	0.25 / 0.19 $n = 12$	0.34 / 0.25 $n = 12$	0.39 / 0.29 $n = 12$	0.24 / 0.18 $n = 12$	0.41 / 0.30 $n = 12$	0.45 / 0.34 $n = 12$
file cut	1.83 / 1.36 $n = 8$	1.06 / 0.80 $n = 8$	1.11 / 0.82 $n = 8$	0.60 / 0.45 $n = 8$	0.61 / 0.46 $n = 8$	0.86 / 0.64 $n = 8$
rasp cut	2.60 / 1.74 $n = 11$	1.33 / 0.85 $n = 11$	1.47 / 1.12 $n = 8$	0.69 / 0.48 $n = 11$	0.74 / 0.54 $n = 11$	1.37 / 1.02 $n = 8$
inverse pyramid pattern	0.68 / 0.51 $n = 10$	0.79 / 0.59 $n = 30$	0.71 / 0.53 $n = 21$	0.50 / 0.38 $n = 10$	0.52 / 0.38 $n = 30$	0.52 / 0.39 $n = 21$
chequered plate	0.66 / 0.48 $n = 13$	0.59 / 0.43 $n = 13$	0.58 / 0.44 $n = 14$	0.65 / 0.48 $n = 13$	0.61 / 0.44 $n = 13$	0.64 / 0.48 $n = 14$
punched geometry 1	-	0.82 / 0.61 $n = 3$	-	-	0.49 / 0.37 $n = 3$	-
punched geometry 2	0.51 / 0.38 $n = 5$	0.48 / 0.36 $n = 5$	0.49 / 0.37 $n = 5$	0.42 / 0.32 $n = 5$	0.43 / 0.32 $n = 5$	0.42 / 0.32 $n = 5$
punched geometry 3	0.80 / 0.60 $n = 10$	0.67 / 0.50 $n = 10$	0.88 / 0.67 $n = 10$	0.61 / 0.45 $n = 10$	0.62 / 0.46 $n = 10$	0.74 / 0.67 $n = 10$
milled circular pattern (steel)	0.58 / 0.44 $n = 12$	0.63 / 0.48 $n = 12$	0.64 / 0.47 $n = 24$	0.41 / 0.31 $n = 12$	0.46 / 0.35 $n = 12$	0.52 / 0.38 $n = 24$
micro notches	1.12 / 0.84 $n = 5$	0.70 / 0.52 $n = 5$	1.29 / 0.97 $n = 5$	0.69 / 0.52 $n = 5$	0.55 / 0.41 $n = 5$	0.96 / 0.71 $n = 5$
milled pyramid pattern 0.5 mm	0.83 / 0.62 $n = 10$	0.87 / 0.65 $n = 40$	0.83 / 0.62 $n = 30$	0.55 / 0.41 $n = 10$	0.56 / 0.42 $n = 40$	0.64 / 0.48 $n = 30$
milled pyramid pattern 1.0 mm	0.89 / 0.67 $n = 20$	0.95 / 0.71 $n = 15$	0.80 / 0.60 $n = 10$	0.54 / 0.40 $n = 20$	0.66 / 0.50 $n = 15$	0.66 / 0.50 $n = 10$
milled pyramid pattern 1.5 mm	1.03 / 0.77 $n = 19$	1.07 / 0.80 $n = 20$	1.06 / 0.80 $n = 18$	0.49 / 0.36 $n = 19$	0.56 / 0.42 $n = 20$	0.44 / 0.33 $n = 18$
milled pyramid pattern 2.0 mm	-	1.12 / 0.83 $n = 12$	-	-	0.83 / 0.62 $n = 12$	-
coated with two-component adhesive and quartz sand (0.5–1.0 mm)	0.75 / 0.57 $n = 4$	0.68 / 0.51 $n = 3$	0.69 / 0.51 $n = 3$	0.66 / 0.50 $n = 4$	0.61 / 0.46 $n = 3$	0.65 / 0.49 $n = 3$
coated with two-component adhesive and quartz sand (0–2 mm)	-	0.64 / 0.48 $n = 3$	0.54 / 0.41 $n = 3$	-	0.41 / 0.31 $n = 3$	0.35 / 0.26 $n = 3$
coated with two-component adhesive and split (2–4 mm)	-	0.61 / 0.46 $n = 3$	0.69 / 0.52 $n = 3$	-	0.38 / 0.28 $n = 3$	0.51 / 0.38 $n = 3$
coated with epoxy resin adhesive tape (0.1 mm) and quartz sand (0–2 mm)	-	0.82 / 0.62 $n = 3$	0.97 / 0.73 $n = 3$	-	0.62 / 0.47 $n = 3$	0.68 / 0.51 $n = 3$
coated with epoxy resin adhesive tape (1.0 mm) and quartz sand (0–2 mm)	-	0.74 / 0.56 $n = 3$	0.82 / 0.61 $n = 3$	-	0.50 / 0.37 $n = 3$	0.61 / 0.46 $n = 3$

FG = face grain and EG = end grain

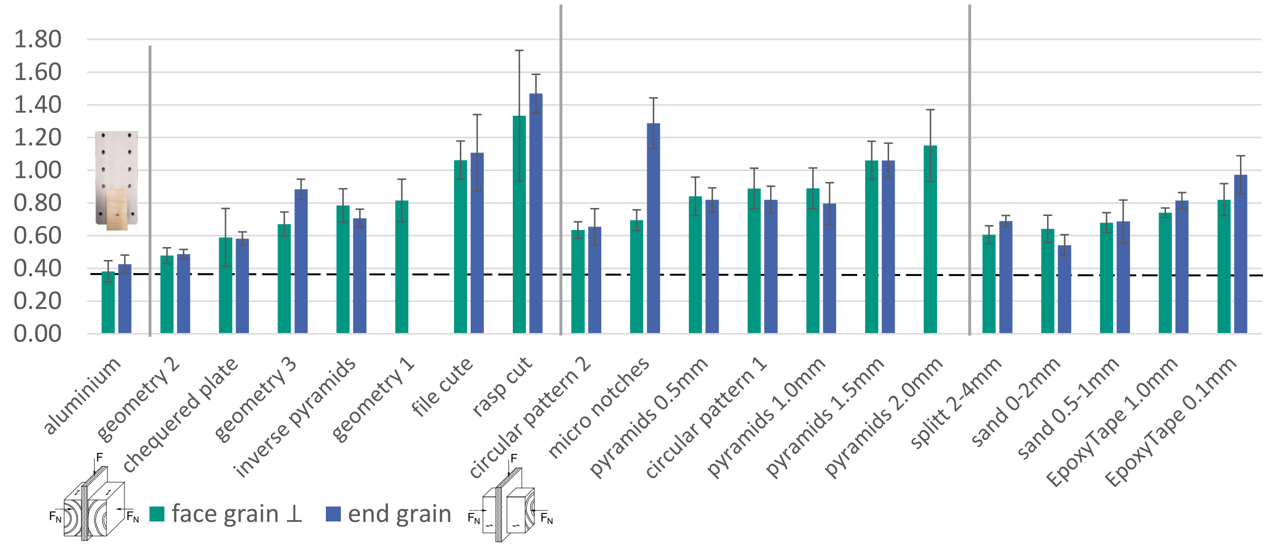

Figure 11: *Overview of test results friction tests.*

3.2 Connection tests

The results for all test series are given in Table 3. The maximum load $F_{V,test}$ (independent of the deformation) and the stiffness k_s (in the range of 10-40 % of the maximum load) was evaluated for all tests. The types of failure observed in the first four test series were either a tensile failure of one or more screws in the shear plane or a withdrawal failure of the screws. In the following, the results of series 1 and series 4 are exemplarily presented and analysed. The results of series 1 with five screws each are shown at the top left of Figure 12. The increase in load-carrying capacity for any surface modification (compared to tests with fasteners without a treated surface) is recognisable and was up to 43 % for the coated surface with quartz sand. Figure 12 also shows that high load-carrying capacities are achieved with surfaces with pronounced structures (analogous to the friction tests). Figure 12 on the top right shows the results for the tests in series 4 with 15 screws. The load-carrying capacity can be increased by up to 30 % compared to the reference tests. Again, a surface with a pronounced structure led to the high increase in load-carrying capacity.

Figure 12 bottom left and right shows the results of the stiffness values. Here, the increase is not as high, only 7 % for series 1 with significantly greater scatter. The stiffness increases with surfaces that have a uniform, even structure. This can be explained by the fact that surfaces with a strong structure are initially pressed into the softwood and absorb deformation. In the case of even, flat surfaces, this is already in full contact and cannot press further into the softwood under load.

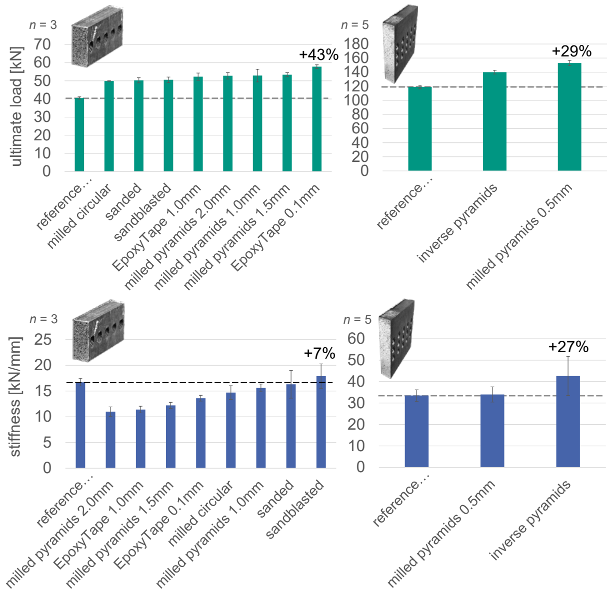

Figure 12: *Test results for series 1 (left) and series 4 (right). Ultimate loads at the top, stiffness values at the bottom.*

In series 5, connectors with screws with a length of 200 mm were tested. Here, for the first time failure of the DVW connector plate itself was observed. The connector failed due to buckling of the veneers when the compressive strength was reached in the net cross-section (Figure 13a). Likewise, compression failure perpendicular to the grain of the softwood below the connector plate was observed for the first time in tests with system connectors (Figure 13b).

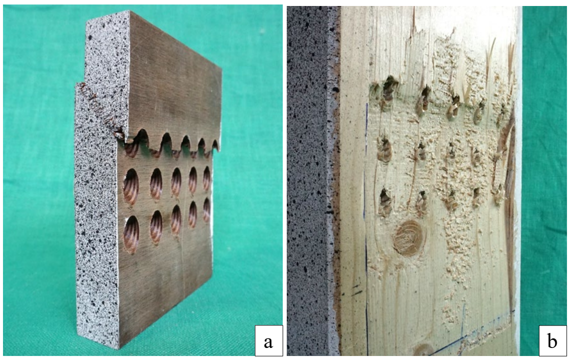

Figure 13: *a) Compressive failure in grain direction of a connector plate and b) compressive failure perpendicular to grain direction of the softwood below the connector plate.*

In the tests of series 6a with the prototype v1 and 10 screws per connector plate, an average maximum load of $F_{V,test} = 151$ kN and an average stiffness of $k_s = 25.0$ kN/mm was achieved. The prototype v2 with 12 screws per connector plate in series 6b achieved an average maximum load of $F_{V,test} = 173$ kN and an average stiffness of $k_s = 33.3$ kN/mm in the tests.

In the first test of series 7, the estimated load could not be achieved because both timber members failed due to compressive failure perpendicular to the grain underneath the connector plates. The test specimens were then reinforced perpendicular to the fibre with fully threaded screws 8x160 mm. In the following, two tests failed due to compression failure of the DVW connector plates, and one test failed due to reaching the tensile load-carrying capacity of the screws. The average ultimate load was $F_{V,test,GLT} = 496$ kN per connector and the corresponding stiffness $k_{s,GLT} = 81$ kN/mm. A final test specimen was made from 5-ply CLT. In the test, only a slightly higher maximum load could be achieved with $F_{V,test,CLT} = 503$ kN. However, the stiffness of the connection could be increased by almost 30 % to $k_{s,CLT} = 105$ kN/mm. Large deformations were observed during the tests. After opening the test specimens, a plastic deformation of the inclined screws was clearly visible, see Figure 14. This explains, among other things, the deviation of the estimated load according to the model from the actual maximum load.

Figure 14: *Plastic deformation of screws 8x300 mm.*

Table 3: *Maximum loads from tests and corresponding stiffnesses (mean values with COV in %).*

series	surface	$F_{V,test}$	k_s
		kN	kN/mm
1	DVW untreated (reference)	40.5 (2%)	16.7 (5%)
	pyramids 1.0 mm	52.9 (8%)	15.6 (5%)
	pyramids 1.5 mm	53.4 (2%)	12.2 (6%)
	pyramids 2.0 mm	52.8 (4%)	11.0 (9%)
	circular pattern	49.9 (0%)	14.7 (10%)
	sanded	50.3 (3%)	16.3 (18%)
	EpoxyTape 0.1mm	57.8 (2%)	13.6 (5%)
	EpoxyTape 1.0mm	52.3 (4%)	11.4 (6%)
2	pyramids 1.0 mm	49.1 (8%)	14.1 (18%)
	pyramids 1.5 mm	47.8 (2%)	15.0 (21%)
3	pyramids 0.5 mm	84.5 (6%)	17.8 (7%)
	circular pattern	80.0 (3%)	17.7 (10%)
4	DVW untreated (reference)	119 (2%)	33.5 (8%)
	embossed pattern	140 (2%)	42.6 (21%)
	pyramids 0.5 mm	153 (3%)	34.0 (10%)
5	embossed pattern	185 (6%)	37.4 (10%)
6a	pyramids 0.5 mm	151 (3%)	25.0 (16%)
6b	pyramids 1.0 mm	173 (5%)	33.3 (7%)
7	pyramids 1.0 mm	496 (1%)	81.0 (5%)

3.3 Analytical model

For comparing the analytical load-carrying capacity $F_{V,exp}$ to the ultimate loads $F_{V,test}$ reached in the tests, the ratio of $F_{V,exp} / F_{V,test}$ was calculated. The comparison resulted in a minimum ratio of 0.75 and an average ratio of 1.10. The average ratios confirm good agreement between the analytical model and the experimental values for the tests, even for significantly higher coefficients of friction. The results are plotted in Figure 15 with green dots for all analytical loads, when using the static coefficient of friction. When using the kinetic coefficient of friction for the model (blue dots in Figure 15), the lowest ratio is 0.92 and the average ratio is 1.28. The evaluation of the coefficient of determination R^2 shows a lower agreement of the model with the test results when using the kinetic coefficient of friction than using the static coefficient of friction.

If the estimated loads are calculated at a characteristic level and a distinction is again made between static and kinetic coefficients of friction, the distribution is as shown in Figure 15 (bottom diagram). In green the results with static coefficient of friction, in blue the results with kinetic coefficient of friction. A distinction was made here between the 5% quantile of the coefficient of friction and the mean value of the coefficient of friction (of a test series). The results show (evaluation of the coefficient of determination R^2) that with the static coefficient of friction there is significantly better agreement between the model and the tests. Furthermore, it can be seen that it makes hardly any difference whether the mean value or the characteristic value of the friction coefficient of a specific surface is used to calculate the estimated load.

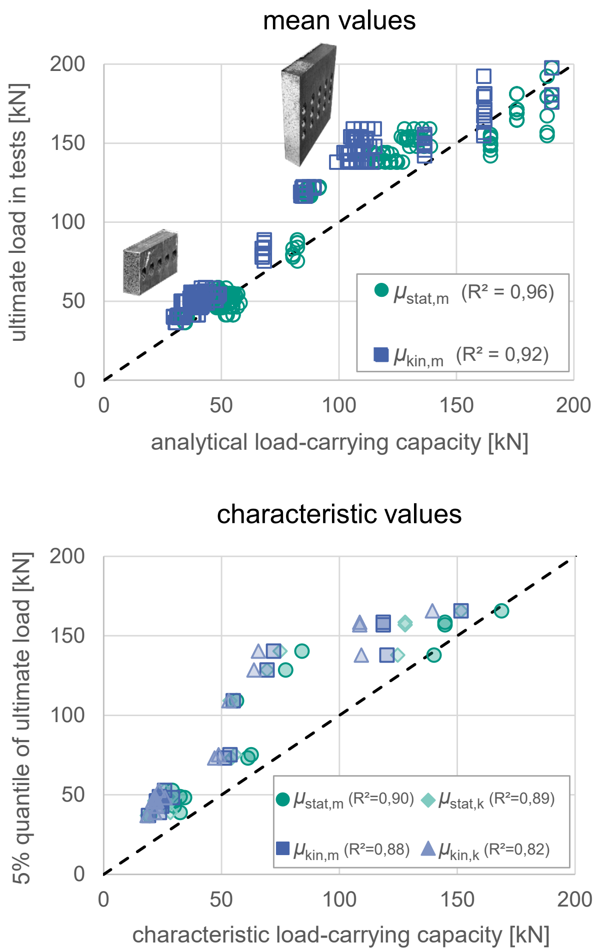

Figure 15: *Comparison of the analytical model with the test results: at the level of mean values (top) and characteristic values (bottom).*

3.4 Long-term behaviour

The test specimens were unloaded after 566 days and allowed to recover for 30 days in the respective service class. This recovery phase was mainly due to logistical reasons in the laboratory. The permanent deformations were between 2.0 and 2.5 mm for connector v1 and about 1.5 mm for connector v2. Immediately before the tests, the test specimens were cut in half in order to obtain the identical push-out test specimens as for the short-term tests. After the tests, the moisture content and the density were determined. The determined moisture content of the test specimens in SC 1 was 10.9% on average, while the moisture content of the test specimens in SC 2 was 15.4% on average.

The connections with connector v2 achieved an average ultimate load of F_{max} = 145 kN in SC 1 and an average ultimate load of 154 kN in SC 2, which corresponds to 84 % and 89 % of the average ultimate load of the short-term tests. Figure 16 (top) shows the results of both the short-term and long-term tests. The decrease in load-carrying capacity compared to the short-term tests can be explained on the one hand by changed or reduced wood properties due to the climatic conditions. On the other hand, shrinkage occurred in the wood in the area of the shear plane and larger deformations had to be applied again until the surface structure completely interlocked with the softwood. The results in SC 2 and the slight decrease in load-carrying capacity show that there was no loss of friction. Here, swelling of the wood led to greater interlocking of the surfaces and thus also to a greater proportion of friction.

The average stiffness of the connectors v2 in SC 1 was k_s = 28.2 kN/mm and was therefore 7% higher than the stiffness of the short-term tests. At 36.4 kN/mm, the stiffness of the connectors in SC 2 was even 9% higher than the short-term tests. Figure 16 (bottom) shows the results of both the short-term and long-term tests. The increase in stiffness in SC 1 confirms the assumption that there was no loss of friction. Due to the constant permanent load, the surface structure was completely pressed into the softwood during the test period and there was no further indentation of the connector plates (which in turn confirms the assumption that a uniform surface structure is advantageous, which does not press into the softwood under load) until at least the load level of the fatigue tests was reached. This is confirmed by the tests in SC 2, in which the swelling of the wood resulted in a stronger interlocking of the surfaces and thus also higher stiffness.

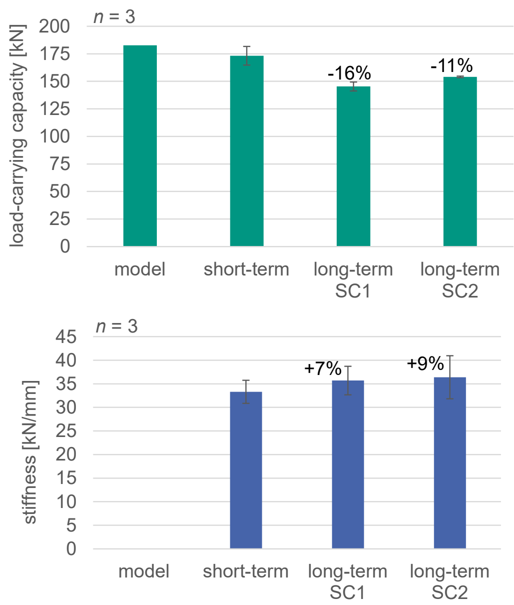

Figure 16: Results of residual capacity and stiffness.

4 SUMMARY AND CONCLUSIONS

4.1 Surface modification

A total of eight different manufacturing processes for different surfaces were analysed. It was found that, on the one hand, simple manufacturing processes lead to large variations in surface quality and, on the other hand, that coatings are associated with a high level of effort but nevertheless very different results in terms of surface quality. Manufacturing processes such as milling or embossing are therefore recommended. Although the processes are more complex and costly, a consistently high surface quality can be guaranteed.

4.2 Friction tests

A total of 26 different surfaces were analysed. All the surface finishes analysed led to significantly higher coefficients of friction in some cases. The most important findings are that strong structuring is not absolutely necessary to achieve a high coefficient of friction. Rather, the uniformity of a surface is of greater importance.

4.3 Connection tests

With the tested surfaces and in combination with inclined fully threaded screws, the load-carrying capacity could be increased by up to 43% and the stiffness by up to 27%. The results showed that surfaces with a strong structure provide good interlocking in softwood and thus increase the load-carrying capacity. On the other hand, surfaces with a flat, uniform structure have a uniform contact in the shear plane from the outset and therefore increase the stiffness.

4.4 Analytical model

The analytical calculation model presented here provides a good representation of the mean values of the load-carrying capacity. When using the static coefficient of friction, the load-carrying capacity tends to be overestimated; when using the kinetic coefficient of friction, it tends to be underestimated. The characteristic load-carrying capacity can also be modelled well using the calculation model. Here, the mean value of the static coefficient of friction is suitable for the design. If the 5% quantile of the static coefficient of friction is used, the results are all on the safe side.

4.5 Long-term behaviour

The storage of the test specimens in two different service classes 1 and 2 showed that the climatic conditions primarily have an influence on the mechanical wood properties and less on the coefficient of friction. For both utilisation classes, it was shown that friction can be activated even after prolonged loading.

REFERENCES

[1] Lagebericht Holzbau 2024, (2024). https://www.holzbau-deutschland.de/fileadmin/user_upload/eingebundene_Downloads/2024-05-06_Lagebericht_2024_lay11_web.pdf (accessed February 28, 2025).

[2] Brancheninfo Bau, (2025). https://www.bauindustrie.de/fileadmin/bauindustrie.de/Zahlen_Fakten/BrancheninfoBau/BiB_-_Baumaterialpreise.pdf (accessed February 28, 2025).

[3] I. Bejtka, H.J. Blaß, Connections with Inclined Screws. Paper 35-7-4, in: Proceedings of CIB W18 - Meeting 35, Kyoto, Japan, 2002.

[4] EN 1995-1-1, Eurocode 5: Design of timber structures – Part 1-1: General – Common rules and rules for buildings; German version, DIN Deutsches Institut für Normung e.V., Berlin, 2012.

[5] S. Aurand, H.J. Blass, Verbinder aus Kunstharzpressholz mit erhöhter Reibung in der Scherfuge, KIT Scientific Publishing, Karlsruhe, 2023.

[6] DIN 8580, Manufacturing processes – Terms and definitions, division, DIN Deutsches Institut für Normung e.V., Berlin, 2022.

[7] T. Schmidt, Kontaktverbindungen für aussteifende Scheiben aus Brettsperrholz, 33 (2018).

[8] EN 14358, Timber structures – Calculation and verification of characteristic values; German version, DIN Deutsches Institut für Normung e.V., Berlin, Berlin, 2016.

[9] EN 14545, Timber structures – Connectors – Requirements; German version, DIN Deutsches Institut für Normung e.V., Berlin, Berlin, 2009.

[10] EN 26891, Timber structures; Connections made with mechanical fasteners; General principles for the determination of strength and deformation characteristic (ISO 6891:1983), DIN Deutsches Institut für Normung e.V., Berlin, Berlin, 1991.